ORGANIC PROCESS RESEARCH & DEVELOPMENT
OPR&D

pubs.acs.org/OPRD

Article

Manufacturing Process Development for Belzutifan, Part 2: A Continuous Flow Visible-Light-Induced Benzylic Bromination

Cecilia Bottecchia,*,⊥ François Lévesque,*,⊥ Jonathan P. McMullen, Yining Ji, Mikhail Reibarkh, Feng Peng, Lushi Tan, Glenn Spencer, Jarod Nappi, Dan Lehnherr, Karthik Narsimhan, Michael K. Wismer, Like Chen, Yipeng Lin, and Stephen M. Dalby

Cite This: https://doi.org/10.1021/acs.oprd.1c00240

ABSTRACT: We report the development and scale-up of a continuous flow photochemical benzylic bromination en route to belzutifan (MK-6482), a small molecule for the treatment of renal cell carcinoma associated with Von Hippel−Lindau syndrome. Compared with the clinical supply route, the photochemical approach circumvents the need for azo radical initiators and proceeds at room temperature. Implementation of continuous flow technology allowed tight control of irradiation and residence time, resulting in a robust process with minimized byproduct formation. This method was selected for the manufacturing process for belzutifan and represents the first commercial continuous flow photochemical process in our company, laying the foundation for the utilization of photochemistry in the pharmaceutical industry.

KEYWORDS: *photochemistry, continuous flow, photobromination, scale-up, manufacturing route development, belzutifan*

Exploiting the energy of light for the generation of highly reactive species is the main principle behind photochemistry and photoredox catalysis.[1,2] Despite the intrinsic synthetic value of these approaches, applications in the pharmaceutical industry have largely been focused on the early stages of drug development, with very few examples showing the implementation of photochemistry beyond the lab scale. In other industries, UV-based photochemical reactions implemented at scale are more common.[3,4] However, because of the prevalence of UV-absorbing chromophores in active pharmaceutical ingredient (API) intermediates, selective activation of substrates with high intensity UV radiation is rare. Moreover, the challenges associated with scale-up are another reason behind the scarcity of photochemical steps in process chemistry: because of the attenuation of light traveling through a medium (as described by the Lambert−Bouguer−Beer law), a scale-up strategy based on the use of increasingly larger vessels is not straightforward.[5] The necessity to source, qualify, and standardize light sources capable of supplying an adequate photon flux to manufacturing reactors represents an additional hurdle toward the implementation of photochemistry in a GMP manufacturing environment. To add to the complexity, operating a photoreactor in a plant setting, where flammable vapors can exist, requires the implementation of suitable safety measures and engineering controls. Advances in reactor design, a deeper understanding of key factors in reaction scale-up,[6] and preinvestment in photochemical capabilities[7] have in recent years brought us closer to realizing the potential of photochemical flow processing for future greener and sustainable manufacturing. Herein we describe the development and implementation of a continuous flow visible-light-induced radical bromination process for the commercial manufacturing process of belzutifan (MK-6482).

Belzutifan is a first-in-class oral hypoxia-inducible factor-2α (HIF-2α) inhibitor for the treatment of certain patients with renal cell carcinoma that received approval by the U.S. Food and Drug Administration in 2021.[8,9] To bring this important new medicine to patients with utmost urgency, a robust and greener commercial manufacturing process for belzutifan was rapidly developed following its acquisition through the purchase of Peloton Therapeutics by Merck & Co., Inc., Kenilworth, NJ, USA in mid-2019.

From a synthetic perspective, belzutifan presents a functionalized indane core bearing a diaryl ether linkage, a methyl sulfone and, most notably, three contiguous stereocenters. The overall commercial manufacturing process, summarized in Scheme 1, proceeds in nine linear steps from the commodity raw material 3,4-dihydrocoumarin. The process development of each step is described in this article (part 2) and the adjoining series of papers (parts 1[10] and 3−6[11−14]).

A key transformation in the clinical supply route for belzutifan comprised a radical benzylic bromination to prepare bromide **2** utilizing indane **1**, 1,3-dibromo-5,5-dimethylhydantoin (DBDMH) as the brominating agent, (Azobisisobutyronitrile) (AIBN) as the radical initiator, and dichloromethane (CH_2Cl_2) as the solvent. The primary drawback of this thermal approach resided in its sensitivity to temperature. A temperature of 40 °C was necessary to initiate the radical mechanism

Special Issue: Excellence in Industrial Organic Synthesis 2021

Received: June 21, 2021

Scheme 1. Overview of the Synthetic Route toward Belzutifan

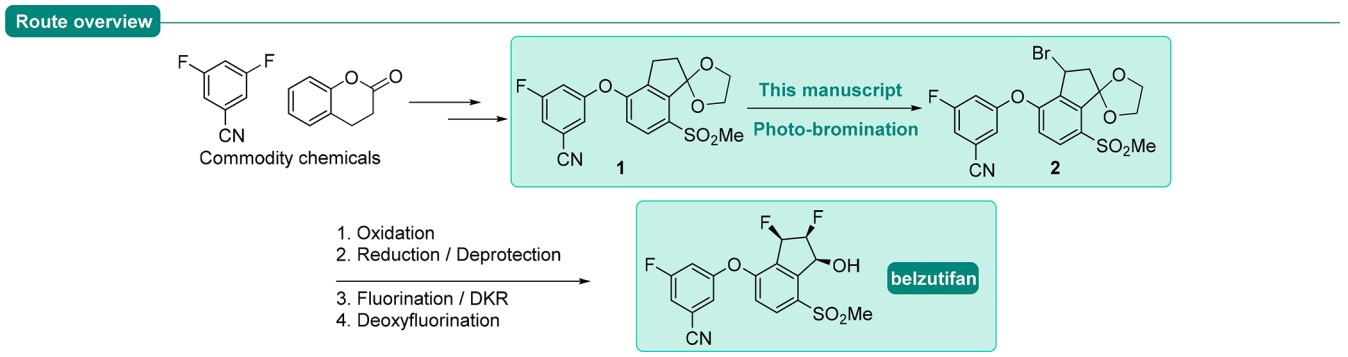

Scheme 2. Process Comparison of the Thermal and Photochemical Approaches to Benzyl Bromide 2

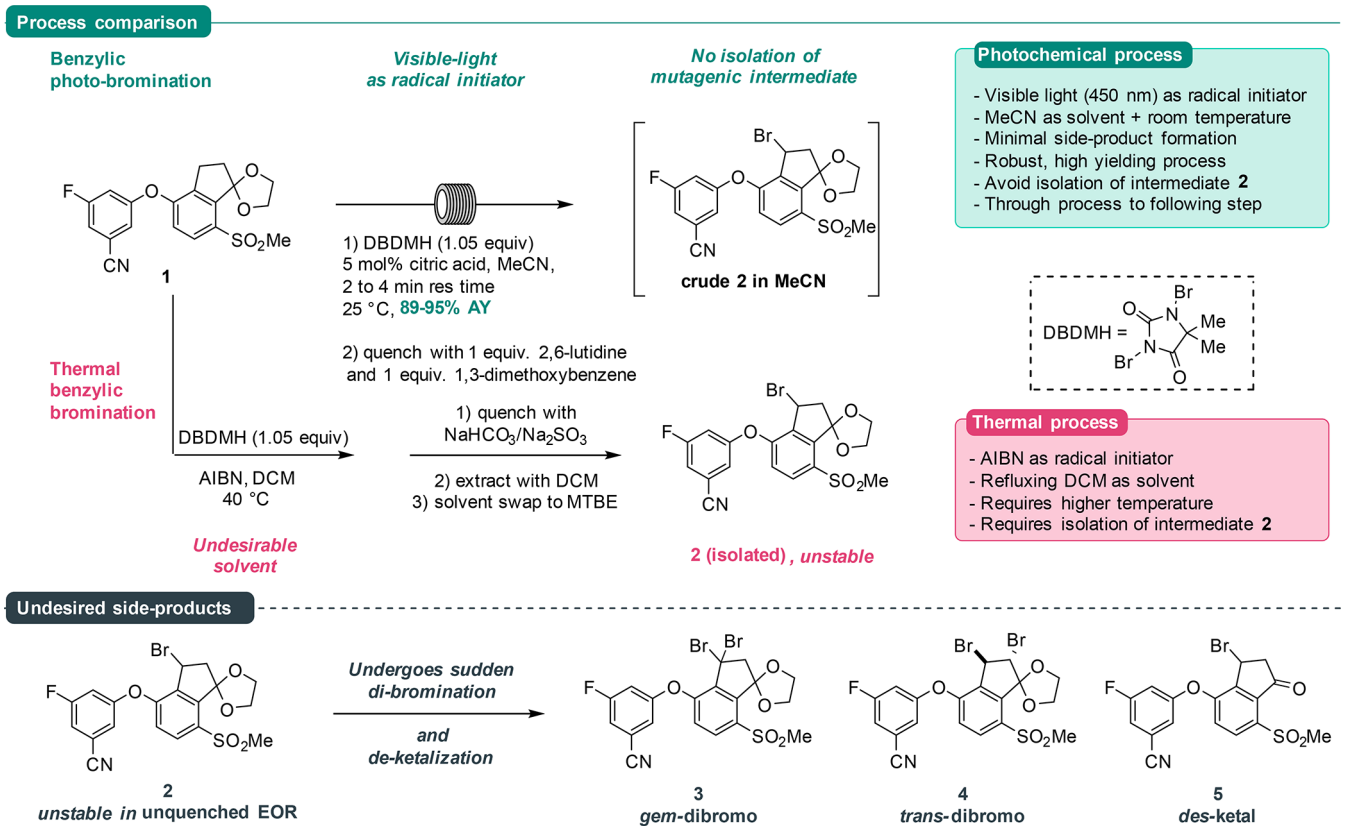

via AIBN decomposition but also impacted the stability of the product. The inability to rapidly and consistently stop the radical reaction via cooling on a large scale triggered uncontrolled overbromination (impurities **3** and **4**) and deketalization (impurity **5**) of the desired product, posing potential batch failure concerns. Moreover, this route required the isolation of intermediate **2**, a compound with poor long-term stability (see Scheme 2). These safety, environmental, and quality concerns rendered this route unsuitable for long-term manufacturing.

To improve the overall robustness and safety of this synthetic step, we investigated the potential to employ light as the radical initiator.[15,16] On the basis of the absorption spectrum of DBDMH (see the Supporting Information), we first attempted to initiate the benzylic bromination of compound **1** with low-intensity 312 nm light. Room-temperature irradiation of a mixture of starting material **1** and DBDMH in 1,2-dichloroethane (DCE) afforded full conversion to the desired product within 1.5 h (Table 1, entry 1; the lamp had 312 nm as its main emission peak). The reaction performed similarly in acetonitrile, albeit under more dilute conditions because of the poor solubility of ketal **1** (Table 1, entry 2). Employment of MeCN also provided the opportunity to perform the bromination and the subsequent oxidation step in the same solvent, obviating the need to isolate bromide **2** with its handling issues.[11,17] Our observation that both a solution of DBDMH in MeCN and the reaction mixture turn orange upon irradiation suggests that DBDMH can slowly release Br_2.[18] Spectroscopic measurements of the irradiated reaction mixture showed significant absorption at 450 nm and good spectral overlap with the absorption profile of Br_2 (see the Supporting Information for spectroscopic data). When blue (i.e., 450 nm) light was employed to initiate the reaction, the desired product was obtained in excellent yield within 3

https://doi.org/10.1021/acs.oprd.1c00240
Org. Process Res. Dev. XXXX, XXX, XXX−XXX

Table 1. Optimization of the Benzylic Photobromination in Batch[a]

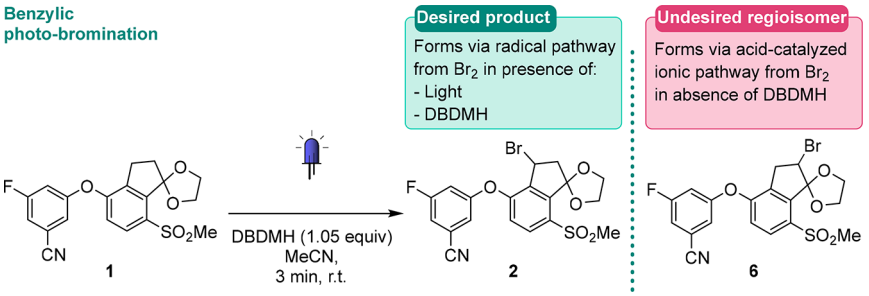

entry	changes from the standard conditions[b]	LCAP[c] of **2**	LCAP of **6**
1	312 nm light, 1.5 h in DCE[d]	89	n.d.[e]
2	312 nm light, 1.5 h	89	n.d.[e]
3	none	91	n.d.[e]
4	Br_2 instead of DBDMH, 450 nm	n.d.[e]	93
5	Br_2 instead of DBDMH, no light	n.d.[e]	92
6	no light	n.d.[e]	n.d.[e]

[a]All reactions were performed on a 200 mg scale of **1** with 1.05 equiv of DBDMH or Br_2. [b]Optimized conditions are as follows: 200 mg of **1**, 1.05 equiv of DBDMH, in 4 mL MeCN. Reaction performed in an M1 Penn photoreactor with 450 nm blue LEDs (3 min of irradiation time total input 3.40 W, 20% intensity, 350 rpm stirring and 5200 rpm cooling fan rate). [c]Liquid chromatography area percent. [d]1,2-Dichloroethane. [e]Not detected.

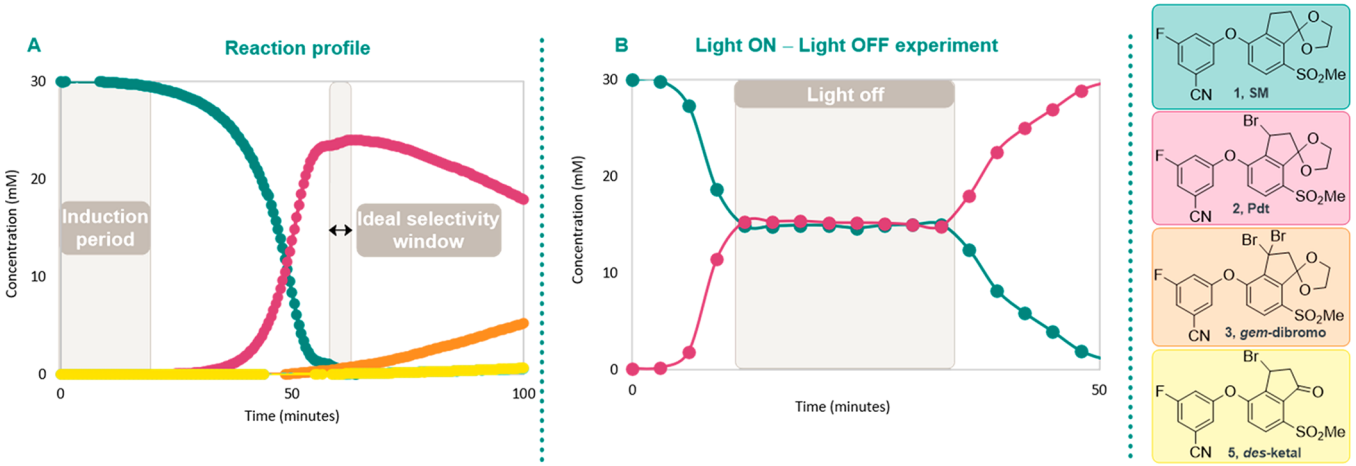

Figure 1. In situ LED−NMR spectroscopy experiments. In both panels, the reaction was performed with starting material **1** (30 mM) and 1.05 equiv of DBDMH in CD_3CN. For more experimental details, refer to the Supporting Information.

min of irradiation (Table 1, entry 3). Literature reports on the mechanism of photochemical benzylic bromination with *N*-bromosuccinimide (NBS) indicate that NBS can release Br_2 and HBr.[19] Similarly, our data suggest that Br_2 is the absorbing species and the brominating agent in our system, with DBDMH serving as a bromine reservoir. This is also in accordance with the work of Goldfinger and co-workers, who identified Br_2 as brominating agent under similar reaction conditions.[20,21] Interestingly, performing the reaction with Br_2 in the absence of DBDMH yielded exclusively the undesired regioisomer **6** (Table 1, entry 4). Our hypothesis for this result is that in the presence of Br_2 alone, bromination at the *β*-position can occur via an ionic mechanism that does not involve the formation of a Br radical. This ionic mechanism requires a catalytic quantity of HBr and proceeds within seconds upon Br_2 addition, thus outcompeting the light-driven radical pathway. An identical result was obtained in the absence of light (Table 1, entry 5), supporting the idea that the formation of regioisomer **6** proceeds via the acid-catalyzed ring-opening equilibrium of the ketal protecting group and does not require irradiation.

Conversely, in the presence of DBDMH, the ionic mechanism is suppressed because DBDMH also acts as a HBr "trap".[20,22] The buffering effect of DBDMH prevents the ring opening of the ketal protecting group. Simultaneously, irradiation of Br_2 results in the formation of Br radicals, which can abstract the benzylic hydrogen in substrate **1**, thus yielding the desired brominated product **2** upon reaction with Br_2. A control experiment with starting material **1** and DBDMH showed that no product formation was observed in the absence of irradiation (Table 1, entry 6).

To further probe our mechanistic hypotheses, we monitored the reaction progress via in situ LED−NMR spectroscopy.[23] This technique allows the combination of in situ light illumination using an optical-fiber-coupled light-emitting diode (LED) and NMR spectroscopy. Although different concentrations and irradiation times are required compared with batch experiments,[24] useful knowledge of the species formed during irradiation can be used to inform process

https://doi.org/10.1021/acs.oprd.1c00240
Org. Process Res. Dev. XXXX, XXX, XXX−XXX

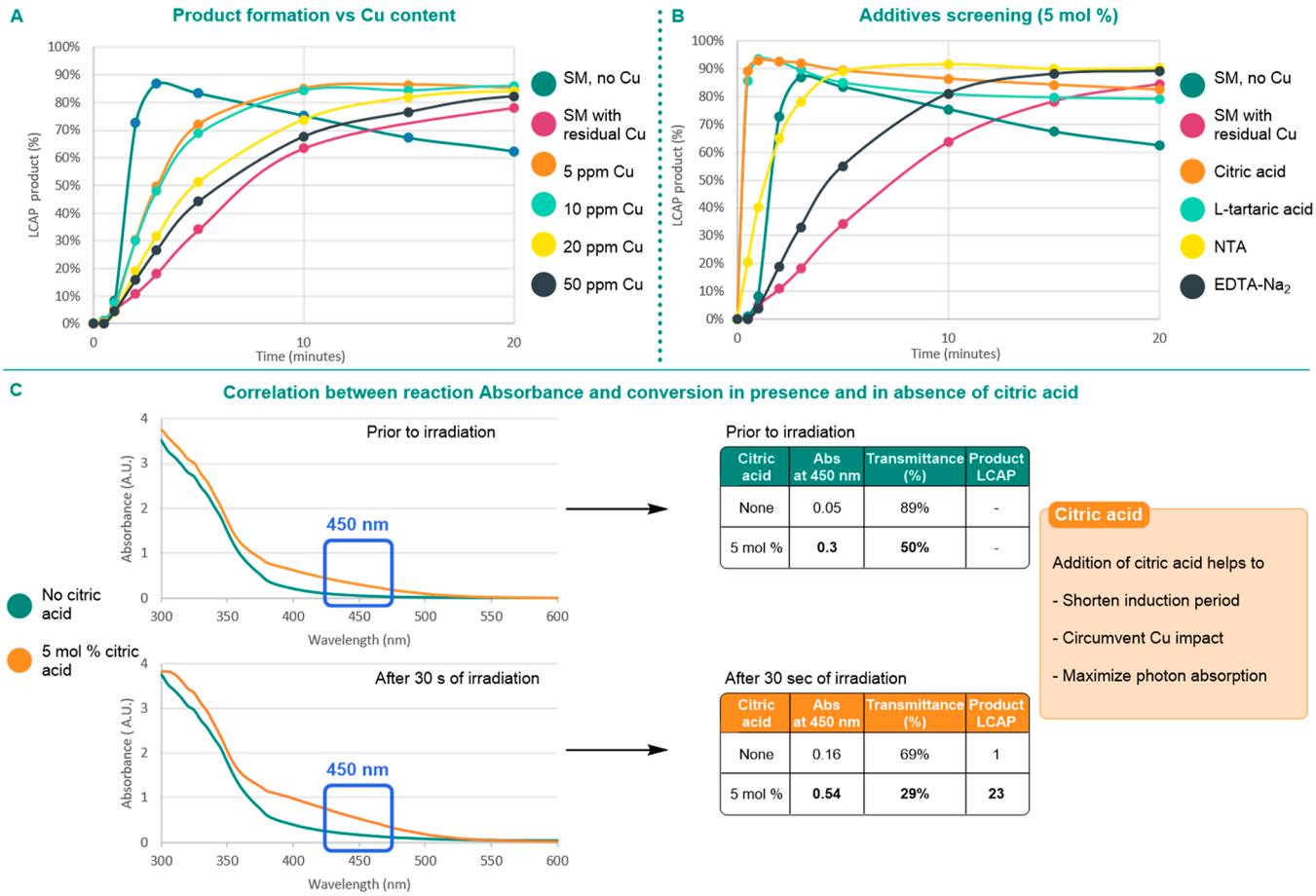

Figure 2. (A) Relationship between the Cu content in starting material **1** and the reaction rate. (B) Impact of additives on the reaction rate. In (A) and (B), the reactions were performed on a 200 mg scale in an Penn Photoreactor M1 with 450 nm blue LEDs (1.05 equiv of DBDMH, 5 mol % additive where applicable, total input 3.40 W, 20% intensity, stirring at 350 rpm, and a 5200 rpm cooling fan rate). (C) Absorbance values for a 22-volume solution of starting material **1** (0.12 M) and 1.05 equiv of DBDMH in MeCN. The comparison is between solutions in the presence and absence of 5 mol % citric acid monohydrate.

development. Figure 1A shows the concentrations of starting material **1** and product **2** over time during irradiation. The reaction profile collected shows an induction period, consistent with the hypothesis that formation of Br_2 from DBDMH is necessary before the reaction can proceed.[25] Past full conversion, the desired product **2** can undergo further radical bromination to yield *gem*-dibromo compound **3**. In an experiment where light irradiation of the reaction mixture was temporally modulated between on and off states (Figure 1B), we observed that the reaction stops in the absence of light, thus confirming the photoinduced nature of this transformation. When a catalytic quantity of Br_2 (5 mol %) was added to a 200 mg scale batch reaction in the presence of DBDMH, disappearance of the induction period was observed, thus supporting the hypothesis that Br_2 is the photoactive species in our system and that its generation is the source of the induction period (for details, see the Supporting Information).

It is worth noting that overbromination to yield byproduct **3** is also a light-catalyzed process, the impact of which can be minimized by appropriate control of the irradiation time. Moreover, on the basis of fate and purge studies in downstream processing, we established the need to run this process at consistent conversion levels and to control the amount of *gem*-dibromo compound **3**. The decision to specifically control the amount of **3** for product quality purposes was also driven by the poor stability of **3**. Upon degradation, this side product eliminates HBr and catalyzes the deprotection of the ketal in the desired product **2**. These considerations support the idea that in order to achieve process robustness, targeting an ideal conversion window would be of great importance. The necessity to tightly control both the reaction and irradiation times, coupled with the practical aspects of photochemistry on scale, pointed us toward the use of a flow reactor to perform this transformation.[26]

Moving from initial results to process development, we evaluated the sensitivity of this chemistry toward impurities and assessed the need to implement adequate control strategies aimed at mitigating any risks. Because of the use of stochiometric quantities of copper in the upstream chemistry[10] and the potential for Cu impurities to be present in starting material **1**, we investigated the impact of this metal on the photobromination reaction rate. The deleterious undesired impact of transition metals on photochemical radical processes is a known drawback of such synthetic approaches and often requires strict purification of starting materials. In our case, we observed that Cu has a significant impact on the reaction rate, suggesting that lot-to-lot variability of the Cu impurity level in starting material **1** may be critical to process robustness. Subjecting a lot of starting material **1** contaminated with 22

https://doi.org/10.1021/acs.oprd.1c00240
Org. Process Res. Dev. XXXX, XXX, XXX−XXX

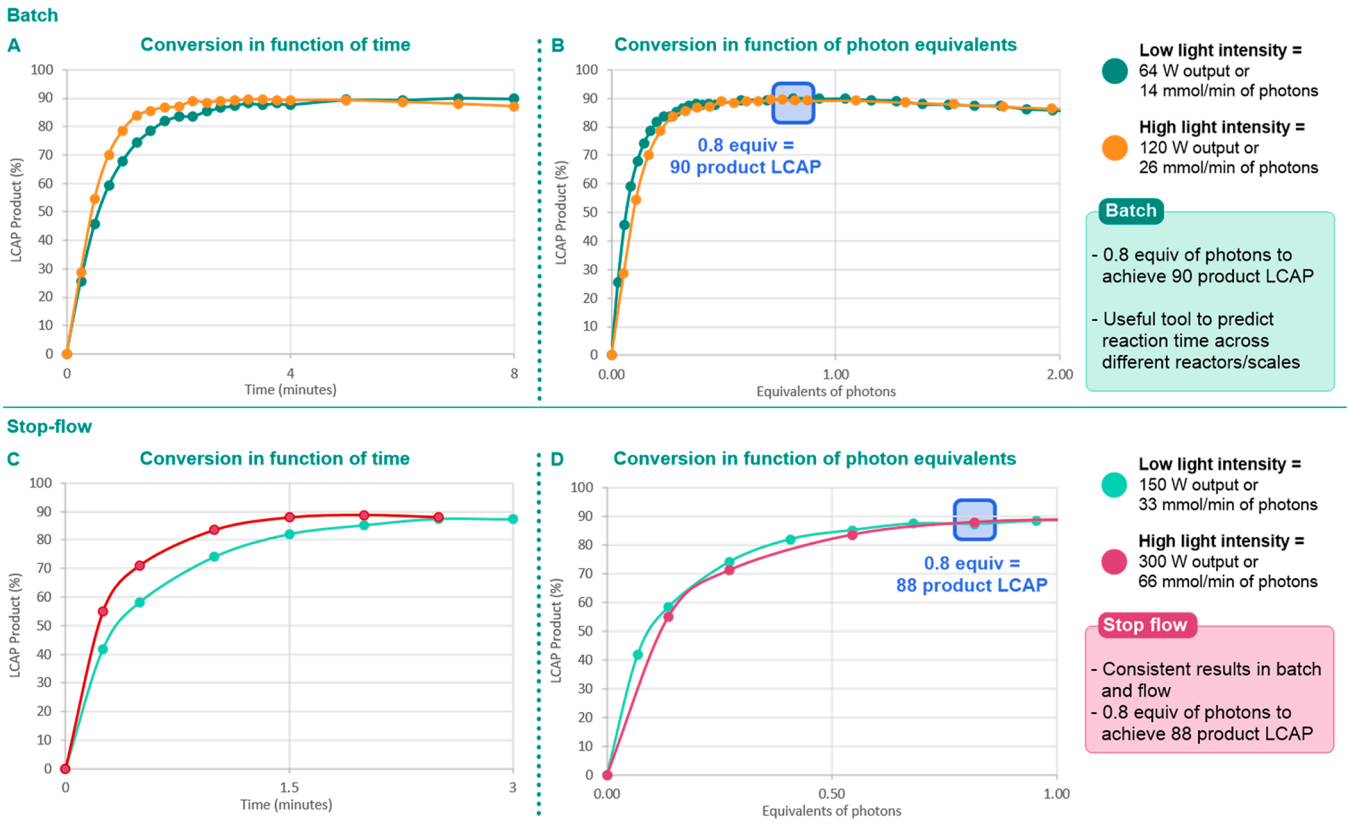

Figure 3. (A, B) Batch experiments: product LCAP as a function of (A) time or (B) number of photon equivalents. The reactions were performed on a 50 g scale with 1.05 equiv of DBDMH and 5 mol % citric acid monohydrate in 22 volumes of MeCN (1.1 L) in a 2 L glass jacketed reactor. The jacket temperature was set to 20 °C, and the reactor was irradiated with four LED chips (64 or 120 W output power) positioned around the vessel. (C, D) Stop flow experiments. Reactions were performed on a 50 g scale with 1.05 equiv of DBDMH and 5 mol % citric acid monohydrate in 20 volumes of MeCN in an 890 mL plug flow reactor. The jacket temperature was set to 10 °C, and the reactor was irradiated with two LED panels (150 or 300 W output power) positioned next to the plug flow reactor.

ppm Cu to irradiation in the presence of DBDMH (1.05 equiv) required a reaction time of 20 min to reach full conversion, as opposed to 3 min in the absence of Cu (Figure 2A, green line vs pink line). To further confirm the relationship between the Cu content in starting material **1** and the reaction rate, we spiked a lot of Cu-free starting material with increasing amounts of CuBr.[27] As depicted in Figure 2A, a direct correlation between the Cu content and the reaction rate was observed.

While upstream controls were implemented to minimize the level of residual copper in compound **1**, the dramatic influence at such low levels necessitated further mitigation. Accordingly, a series of known copper chelators were screened as potential additives to our system (for a full list of additives tested, see the Supporting Information). As depicted in Figure 2B, both ethylenediaminetetraacetic acid (EDTA) and nitrilotriacetic acid (NTA) emerged as feasible additives to restore an initial reaction rate comparable to what was observed in the absence of Cu. Further screening focusing on alkyl compounds with multiple carboxylic acid moieties allowed us to identify citric acid and L-tartaric acid as inexpensive and readily available additives. The positive effect on the reaction rate observed in the presence of citric acid surpassed what we had observed with NTA (Figure 2B). This result and the observation that the absorbance of the reaction mixture at 450 nm increased in the presence of citric acid monohydrate even prior to irradiation suggested that this additive favors the generation of Br_2 from DBDMH (Figure 2C). An increased initial reaction rate and disappearance of the induction period in the presence of 5 mol % citric acid further served to corroborate this hypothesis (Figure 2C).

With the citric acid additive identified, we determined the need for an additional control strategy based on the performance of different lots of starting material **1**, which we attributed to unknown impurities that absorb light at 450 nm. In contaminated batches, the presence of such impurities resulted in unproductive photon absorption and the need for extended reaction times. We thus implemented a carbon treatment of this substrate (activated carbon, 5−10 wt % loading relative to starting material **1**) and set acceptable absorption values for the carbon-treated solution of compound **1** (see the Supporting Information for additional information). This control strategy proved to be effective in standardizing the reaction performance against lot-to-lot variability.

In parallel to the reaction optimization, various quenches to prevent the need for isolation of the desired product were examined. The key goal was to ensure that the quenched reaction stream could be used directly in the subsequent synthetic step. This investigation led to the identification of quenching conditions involving the use of neat 2,6-lutidine and 1,3-dimethoxybenzene. The presence of 2,6-lutidine neutralized any trace of HBr present in the reaction stream, and 1,3-dimethoxybenzene reacted with any residual electrophilic bromine (Br^+). This approach proved to be useful in improving the long-term stability of the product in the reaction stream, which could then be carried into the following

https://doi.org/10.1021/acs.oprd.1c00240
Org. Process Res. Dev. XXXX, XXX, XXX−XXX

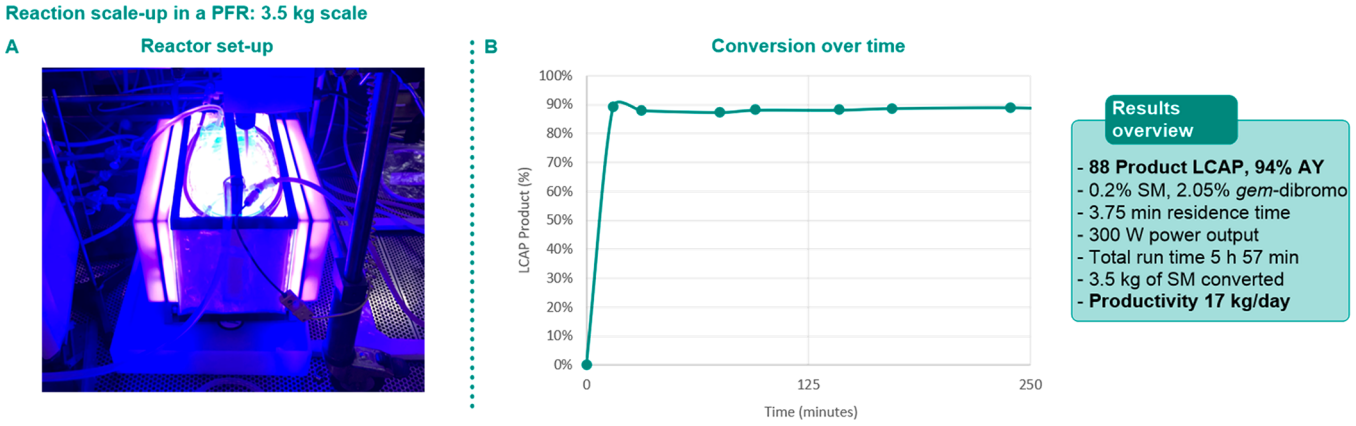

Figure 4. Overview of scale-up in a tubular PFR. (A) Photograph of the reactor immersed in a fish tank and irradiated with two LED panels. For setup details and procedure, see the Supporting Information. (B) Product conversion over time and a table showing an overview of the results.

oxidation step without the need for product isolation (for more details on the reaction quench and oxidation step, see ref 11).

Having optimized the reaction conditions and the quenching procedure, we then focused our efforts on scaling this photochemical process. Previous endeavors by our group had shown that the number of photon equivalents can serve as an effective scaling factor to predict photochemical reaction performance across scales and reactors.[6] In other words, as long as a given reaction operates under a photon-limited regime and efficient heat and mass transfer are ensured, the number of photon equivalents necessary to drive the reaction to full conversion remains the same for every reactor geometry or photon flux.

This statement can be demonstrated by comparing the reaction profiles obtained in a 1 L batch reactor irradiated at different light intensities (i.e., 64 or 120 W output) (Figure 3). When the product liquid chromatography area percents (LCAPs) from different experiments were plotted as functions of time (Figure 3), poor profile overlap due to the difference in photon fluxes was observed. Conversely, plotting the product LCAP as a function of photon equivalents emitted by the light source[28] results in good profile overlap (Figure 3).[29] In both instances, delivering 0.8 equiv of photons to this reactor resulted in the same product yield (90 LCAP), although the times necessary for those photons to be emitted are different (7 min at 64 W output vs 3.5 min at 120 W output).

A direct consequence of the higher absorbance of reaction mixtures containing citric acid is an overall improvement in productive photon capture by the system. In other words, citric acid maximizes photon absorbance by increasing the Br_2 concentration at the beginning of the reaction, resulting in a more productive use of photons delivered by the light source (Figure 2C). This focus on photon capture is especially relevant when considering the use of a continuous plug flow reactor (PFR) to further scale up this chemistry, as these reactors usually rely on the use of small-diameter tubing and therefore have short path lengths. The tight control of the irradiation time and the narrow residence time distribution typical of a PFR are instrumental in ensuring the high conversion and minimal formation of *gem*-dibromo impurity **3** required to meet our process purity specifications.

We recently constructed a small-footprint tubular PFR optimized for increased photon absorption through the appropriate choice of tubing diameter, light source, and reactor geometry.[7,30] The tubular reactor (8 mm i.d., 890 mL volume) is housed in a 20.8 L glass aquarium tank and is irradiated with two panels of LEDs, each consisting of 15 high-intensity blue LED chips mounted on an aluminum heat sink (for more details, see the Supporting Information). Employing this setup, we investigated the photon stoichiometry as well as the impact of the light intensity on our system. In order to minimize the amount of materials necessary for the experiment, we employed a stop flow approach.[31]

On the basis of the results obtained in the 1 L batch scale-up (Figure 3B), we anticipated that the same number of photon equivalents would be necessary to achieve the desired product LCAP. At power outputs of 150 and 300 W, 0.8 equiv of photons would correspond to reaction times of 3 and 1.5 min, respectively. The results obtained were well in line with our predictions: 0.8 equiv of photons resulted in 88 product LCAP at both light intensities. The highest product LCAP (89) was achieved at both light intensities with 1 equiv of photons (Figure 3D, compared with the batch result depicted in Figure 3B).

Employing the same PFR, we demonstrated this transformation on a kilogram scale in our kilo-lab facility. A solution of starting material **1**, DBDMH, and 5 mol % citric acid was prepared and fed into the PFR via a peristaltic pump. With a residence time of 3.75 min and a 2 × 500 W total power input, 3.25 kg of starting material **1** was converted to the desired product **2** in approximately 6 h (0.22% **1**, 2.2% *gem*-dibromo impurity **3**, and 88 LCAP **2**, corresponding to an assay yield of 94%) (Figure 4; see the Supporting Information for additional details). Upon exiting the reactor, the reaction stream was flowed into a second vessel containing a quench solution of neat 2,6-lutidine and 1,3-dimethoxybenzene. Throughout the run, temperature control was maintained by water cooling of both the LED panels and the reactor.

Achieving a productivity comparable to that of the alternative thermal radical process toward the desired product **2** was an essential requirement to enable the implementation of this photochemical approach on the manufacturing scale. To date, attaining productivities in the range of hundreds of kilograms per day with a continuous flow photochemical reactor has represented a challenge.[32−34] With our initial system, a productivity of 17 kg/day was achieved. To match the required productivity for this intermediate and to build a system that can be operated in a manufacturing environment, we focused our attention on the development of a second-generation tubular PFR. A tubular reactor (0.83 L, 7.1 mm i.d.)

https://doi.org/10.1021/acs.oprd.1c00240
Org. Process Res. Dev. XXXX, XXX, XXX−XXX

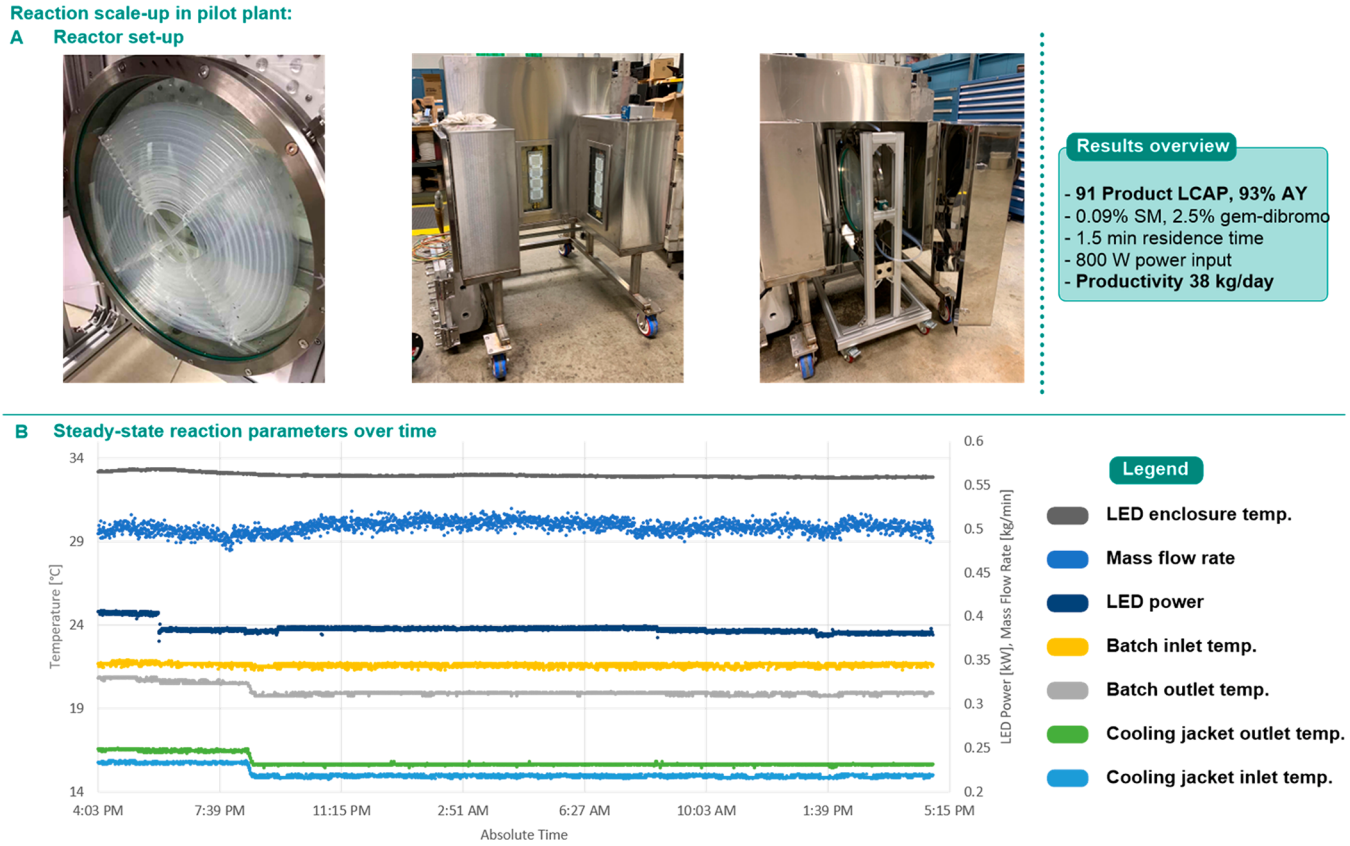

Figure 5. Overview of scale-up in a tubular PFR in the pilot plant. (A) From left to right: close-up of the tubular reactor in its housing and surrounded by cooling liquid, the LED skid, and the tubular reactor positioned within the LED skid. (B) Steady-state reaction parameters over time, including temperatures at different positions, the LED power, and the mass flow rate over an extended run. The batch inlet and outlet temperatures are the temperatures of the reaction stream upon entering and exiting the flow reactor.

was coiled in a spiral fashion and housed within two glass plates (Figure 5A). The glass plates were connected to form an enclosure that simultaneously housed the reactor and allowed for recirculation of cooling fluid. High-intensity LED chips were mounted on a separate metal enclosure surrounding the reactor unit (see Figure 5A and additional details in the Supporting Information).

This reactor assembly was employed to convert 50 kg of starting material **1** to the desired product **2** in our pilot-plant facility in 32 h of processing time, thus bringing the productivity of this system to 38 kg/day (Figure 5B). Results similar to those from the preparatory lab scale-up were obtained (0.09% **1**, 2.5% *gem*-dibromo impurity **3**, and 91 LCAP **2**, corresponding to an assay yield of 93%, with a residence time of 1.5 min and a total power input of 800 W; see the Supporting Information for additional details). Excellent stability in terms of conversion was observed, and the temperature and LED performance were maintained throughout the run (Figure 5; see the Supporting Information for details on the reactor and the setup process flow diagram).

On the basis of the productivity obtained with the pilot-plant reactor, we estimated that a numbering-up approach with several of the described reactor units connected in series would allow us to attain suitable productivity. We thus built a Good Manufacturing Practice (GMP)-qualified reactor train meeting all of the safety requirements for operation in a plant setting. The same reactor units were employed, and each reactor was irradiated with two LED panels. An inline quench was also introduced, allowing the rection mixture flowing out of the last photoreactor unit to be quenched in situ. With this optimized setup, a productivity of >100 kg/day was achieved (0.03% **1**, 2.0% *gem*-dibromo impurity **3**, and 91 LCAP **2**, corresponding to an assay yield of 94%, with a residence time of 3 min). Multiple successful scale-up campaigns followed these initial results, and overall, more than 1 ton of the desired product **2** was produced with this photochemical setup and successfully through-processed into the subsequent oxidation step. Furthermore, the employment of these new photochemical reactors provided a solution to the long-standing challenge of translating bench-scale photochemistry to a manufacturing setting.

In conclusion, we have described the development of a photochemical benzylic bromination en route to MK-6482. This photoflow approach enabled improved safety and robustness compared with the alternative thermal process. In situ LED−NMR spectroscopy experiments were used to gain a better understanding of reaction mechanism and selectivity. The use of substochiometric citric acid enabled reaction rate enhancement by decreasing the induction period as well as alleviating lot-to-lot variability due to parts per million levels of Cu impurities. Photon stoichiometry was employed as a useful tool to predict the reaction times at different light intensities and in different setups. Employing a tubular plug flow reactor, we demonstrated this chemistry on a multikilogram scale. The precise control over irradiation and temperature as well as the narrow residence time distribution afforded excellent selectivity for the desired product. Technology transfer and further development culminated in the design of a manufacturing PFR

https://doi.org/10.1021/acs.oprd.1c00240
Org. Process Res. Dev. XXXX, XXX, XXX−XXX

tubular reactor that was employed to synthesize product **2** under GMP conditions. In so doing, we have established an elegant solution to the scale-up of photochemical processes and expect that the photochemical renaissance of the past 10–15 years will now pay dividends in the utilization of this technology in the manufacture of APIs.

■ ASSOCIATED CONTENT

Supporting Information

The Supporting Information is available free of charge at https://pubs.acs.org/doi/10.1021/acs.oprd.1c00240.

Experimental procedures, spectroscopic data, additives screened, and setup details (PDF)

■ AUTHOR INFORMATION

Corresponding Authors

Cecilia Bottecchia − *Process Research & Development, Merck & Co., Inc., Rahway, New Jersey 07065, United States;* orcid.org/0000-0003-3355-1805; Email: cecilia.bottecchia@merck.com

François Lévesque − *Process Research & Development, Merck & Co., Inc., Rahway, New Jersey 07065, United States;* Email: francois.levesque@merck.com

Authors

Jonathan P. McMullen − *Process Research & Development, Merck & Co., Inc., Rahway, New Jersey 07065, United States;* orcid.org/0000-0001-5969-2396

Yining Ji − *Analytical Research & Development, Merck & Co., Inc., Rahway, New Jersey 07065, United States;* orcid.org/0000-0002-9650-6844

Mikhail Reibarkh − *Analytical Research & Development, Merck & Co., Inc., Rahway, New Jersey 07065, United States;* orcid.org/0000-0002-6589-707X

Feng Peng − *Process Research & Development, Merck & Co., Inc., Rahway, New Jersey 07065, United States;* orcid.org/0000-0002-2382-2862

Lushi Tan − *Process Research & Development, Merck & Co., Inc., Rahway, New Jersey 07065, United States*

Glenn Spencer − *Process Research & Development, Merck & Co., Inc., Rahway, New Jersey 07065, United States*

Jarod Nappi − *Process Research & Development, Merck & Co., Inc., Rahway, New Jersey 07065, United States*

Dan Lehnherr − *Process Research & Development, Merck & Co., Inc., Rahway, New Jersey 07065, United States;* orcid.org/0000-0001-8392-1208

Karthik Narsimhan − *Process Research & Development, Merck & Co., Inc., Rahway, New Jersey 07065, United States*

Michael K. Wismer − *Scientific Engineering & Design, Merck & Co., Inc., Kenilworth, New Jersey 07033, United States*

Like Chen − *Shanghai SynTheAll Pharmaceutical Co. Ltd., Shanghai 201507, China*

Yipeng Lin − *Shanghai SynTheAll Pharmaceutical Co. Ltd., Shanghai 201507, China*

Stephen M. Dalby − *Process Research & Development, Merck & Co., Inc., Rahway, New Jersey 07065, United States*

Complete contact information is available at: https://pubs.acs.org/10.1021/acs.oprd.1c00240

Author Contributions

[⊥]C.B. and F.L. contributed equally. All of the authors approved the final version of the manuscript.

Notes

The authors declare no competing financial interest.

■ ACKNOWLEDGMENTS

We thank Dr. Gregory Pirrone, Bangping Xiang, and Ryan Peters for their analytical support and Dr. Sean Dubina and Adam Fine for their support with process characterization. We are grateful to Daniel Bishara, Anna Jenks, Ted Furman, and all of the operators for their support during the reaction scale-up in the pilot plant and to Vito Rapisardi and Lisa Frey for their help with scale-up work in the preparatory laboratory facility. Finally, we thank Dr. John Naber for helpful discussions. All of the acknowledged individuals were affiliated with Merck & Co., Inc. (Kenilworth, NJ, USA) at the time of their contributions.

■ REFERENCES

(1) Prier, C. K.; Rankic, D. A.; MacMillan, D. W. C. Visible Light Photoredox Catalysis with Transition Metal Complexes: Applications in Organic Synthesis. *Chem. Rev.* **2013**, *113* (7), 5322−5363.

(2) Romero, N. A.; Nicewicz, D. A. Organic Photoredox Catalysis. *Chem. Rev.* **2016**, *116* (17), 10075−10166.

(3) Fischer, M. Industrial Applications of Photochemical Syntheses. *Angew. Chem., Int. Ed. Engl.* **1978**, *17* (1), 16−26.

(4) Turconi, J.; Griolet, F.; Guevel, R.; Oddon, G.; Villa, R.; Geatti, A.; Hvala, M.; Rossen, K.; Göller, R.; Burgard, A. Semisynthetic Artemisinin, the Chemical Path to Industrial Production. *Org. Process Res. Dev.* **2014**, *18* (3), 417−422.

(5) Donnelly, K.; Baumann, M. Scalability of photochemical reactions in continuous flow mode. *J. Flow Chem.* **2021**, *11*, 223−241.

(6) Corcoran, E. B.; McMullen, J. P.; Lévesque, F.; Wismer, M. K.; Naber, J. R. Photon Equivalents as a Parameter for Scaling Photoredox Reactions in Flow: Translation of Photocatalytic C-N Cross-Coupling from Lab Scale to Multikilogram Scale. *Angew. Chem., Int. Ed.* **2020**, *59* (29), 11964−11968.

(7) Lévesque, F.; Di Maso, M. J.; Narsimhan, K.; Wismer, M. K.; Naber, J. R. Design of a Kilogram Scale, Plug Flow Photoreactor Enabled by High Power LEDs. *Org. Process Res. Dev.* **2020**, *24* (12), 2935−2940.

(8) Xu, R.; Wang, K.; Rizzi, J. P.; Huang, H.; Grina, J. A.; Schlachter, S. T.; Wang, B.; Wehn, P. M.; Yang, H.; Dixon, D. D.; Czerwinski, R. M.; Du, X.; Ged, E. L.; Han, G.; Tan, H.; Wong, T.; Xie, S.; Josey, J. A.; Wallace, E. M. 3-[(1*S*,2*S*,3*R*)-2,3-Difluoro-1-hydroxy-7-methylsulfonylindan-4-yl]oxy-5-fluorobenzonitrile (PT2977), a Hypoxia-Inducible Factor 2α (HIF-2α) Inhibitor for the Treatment of Clear Cell Renal Cell Carcinoma. *J. Med. Chem.* **2019**, *62* (15), 6876−6893.

(9) Choueiri, T. K.; Motzer, R. J. Systemic Therapy for Metastatic Renal-Cell Carcinoma. *N. Engl. J. Med.* **2017**, *376* (4), 354−366.

(10) Peng, F.; Tan, L.; Chen, L.; Dalby, S. M.; DiRocco, D. A.; Duan, J.; Feng, M.; Gong, G.; Guo, H.; Hethcox, J. C.; Jin, L.; Johnson, H. C.; Kim, J.; Le, D.; Lin, Y.; Liu, W.; Shen, J.; Wan, Y.; Xiao, C.; Xiang, B.; Xiang, Q.; Xu, J.; Yan, L.; Yang, W.; Ye, H.; Yu, Y.; Zhang, J. Manufacturing Process Development for Belzutifan, Part 1: A Concise Synthesis of the Indanone Starting Material. *Org. Process Res. Dev.* **2021**, DOI: 10.1021/acs.oprd.1c00236.

(11) Chen, Z.; Salehi Marzijarani, N.; Quirie, S.; Pirrone, G. F.; Dalby, S. M.; Wang, T.; Kim, J.; Peng, F.; Fine, A. J. Manufacturing Process Development for Belzutifan, Part 3: Completing a Streamlined Through-Process with a Safe and Scalable Oxidation. *Org. Process Res. Dev.* **2021**, DOI: 10.1021/acs.oprd.1c00232.

(12) Salehi Marzijarani, N.; Fine, A. J.; Dalby, S. M.; Gangam, R.; Poudyal, S.; Behre, T.; Ekkati, A. R.; Armstrong, B. A.; Shultz, C. S.; Dance, Z. E. X.; Stone, K. Manufacturing Process Development for Belzutifan, Part 4: Nitrogen Flow Criticality for Transfer Hydrogenation Control. *Org. Process Res. Dev.* **2021**, DOI: 10.1021/acs.oprd.1c00231.

(13) Wang, T.; Phillips, E. M.; Dalby, S. M.; Sirota, E.; Axnanda, S.; Shultz, C. S.; Patel, P.; Waldman, J. H.; Alwedi, E.; Wang, X.; Zawatzky, K.; Chow, M.; Padivitage, N.; Weisel, M.; Whittington, M.; Duan, J.; Lu, T. Manufacturing Process Development for Belzutifan, Part 5: A Streamlined Fluorination−Dynamic Kinetic Resolution Process. *Org. Process Res. Dev.* **2021**, DOI: 10.1021/acs.oprd.1c00242.
(14) Pirnot, M.; Stone, K.; Wright, T. J.; Lamberto, D. J.; Schoell, J.; Lam, Y.-h.; Zawatzky, K.; Wang, X.; Dalby, S. M.; Fine, A. J.; McMullen, J. P. Manufacturing Process Development for Belzutifan, Part 6: Ensuring Scalability for a Deoxyfluorination Reaction. *Org. Process Res. Dev.* **2021**, DOI: 10.1021/acs.oprd.1c00239.
(15) Chen, M.; Zhong, M.; Johnson, J. A. Light-Controlled Radical Polymerization: Mechanisms, Methods, and Applications. *Chem. Rev.* **2016**, *116* (17), 10167−10211.
(16) Cantillo, D.; de Frutos, O.; Rincon, J. A.; Mateos, C.; Kappe, C. O. A Scalable Procedure for Light-Induced Benzylic Brominations in Continuous Flow. *J. Org. Chem.* **2014**, *79* (1), 223−229.
(17) Alfonsi, K.; Colberg, J.; Dunn, P. J.; Fevig, T.; Jennings, S.; Johnson, T. A.; Kleine, H. P.; Knight, C.; Nagy, M. A.; Perry, D. A.; Stefaniak, M. Green chemistry tools to influence a medicinal chemistry and research chemistry based organisation. *Green Chem.* **2008**, *10* (1), 31−36.
(18) Bonfield, H. E.; Williams, J. D.; Ooi, W. X.; Leach, S. G.; Kerr, W. J.; Edwards, L. J. A Detailed Study of Irradiation Requirements Towards an Efficient Photochemical Wohl-Ziegler Procedure in Flow. *ChemPhotoChem.* **2018**, *2* (10), 938−944.
(19) Incremona, J. H.; Martin, J. C. N-bromosuccinimide. Mechanisms of allylic bromination and related reactions. *J. Am. Chem. Soc.* **1970**, *92* (3), 627−634.
(20) Adam, J.; Gosselain, P. A.; Goldfinger, P. Laws of Addition and Substitution in Atomic Reactions of Halogens. *Nature* **1953**, *171* (4355), 704−705.
(21) Djerassi, C. Brominations with *N*-Bromosuccinimide and Related Compounds. The Wohl−Ziegler Reaction. *Chem. Rev.* **1948**, *43* (2), 271−317.
(22) Ji, Y.; Bottecchia, C.; Lévesque, F.; Narsimhan, K.; Lehnherr, D.; McMullen, J. P.; Dalby, S. M.; Xiao, K.-J.; Reibarkh, M. Benzylic Photobromination for the Synthesis of Belzutifan: Elucidation of Reaction Mechanisms Using In Situ LED-NMR. *J. Org. Chem.* **2021**, DOI: 10.1021/acs.joc.1c01465.
(23) Ji, Y.; DiRocco, D. A.; Kind, J.; Thiele, C. M.; Gschwind, R. M.; Reibarkh, M. LED-Illuminated NMR Spectroscopy: A Practical Tool for Mechanistic Studies of Photochemical Reactions. *ChemPhotoChem.* **2019**, *3* (10), 984−992.
(24) Requiring different irradiation times is not unexpected, as different numbers of photons per mole of starting material impinge on the reaction mixture, the ratios of illuminated surface area to volume are different, and different light intensities are used.
(25) Goldfinger, P.; Gosselain, P. A.; Martin, R. H. Induction Periods in Reactions of N-Halogenimides. *Nature* **1951**, *168* (4262), 30−32.
(26) Cambié, D.; Bottecchia, C.; Straathof, N. J. W.; Hessel, V.; Noël, T. Applications of Continuous-Flow Photochemistry in Organic Synthesis, Material Science, and Water Treatment. *Chem. Rev.* **2016**, *116* (17), 10276−10341.
(27) CuBr was selected as the copper source because it was used in the upstream chemistry.
(28) Emitted photons are photons emitted at the surface of the light source, including photons that might not be absorbed by our reactor because of diffusion or diffraction. Because of the similar reactor geometries, the differences between the numbers of emitted and absorbed photons should be similar.
(29) For details on calculations of the number of photon equivalents, see the Supporting Information.
(30) Leblebici, M. E.; Van den Bogaert, B.; Stefanidis, G. D.; Van Gerven, T. Efficiency vs. productivity in photoreactors, a case study on photochemical separation of Eu. *Chem. Eng. J.* **2017**, *310*, 240−248.
(31) Stop flow refers to charging the reactor with the reaction mixture, performing irradiation, and emptying the reactor to obtain a homogeneous mixture. The irradiated mixture was recharged into the reactor, and the sequence was repeated. By the use of this stop flow method, the minimal amount of material was used to collect a full reaction profile.
(32) Steiner, A.; Roth, P. M. C.; Strauss, F. J.; Gauron, G.; Tekautz, G.; Winter, M.; Williams, J. D.; Kappe, C. O. Multikilogram per Hour Continuous Photochemical Benzylic Brominations Applying a Smart Dimensioning Scale-up Strategy. *Org. Process Res. Dev.* **2020**, *24*, 2208−2216.
(33) Steiner, A.; Williams, J. D.; de Frutos, O.; Rincón, J. A.; Mateos, C.; Kappe, C. O. Continuous photochemical benzylic bromination using in situ generated Br2: process intensification towards optimal PMI and throughput. *Green Chem.* **2020**, *22* (2), 448−454.
(34) Beaver, M. G.; Zhang, E.-x.; Liu, Z.-q.; Zheng, S.-y.; Wang, B.; Lu, J.-p.; Tao, J.; Gonzalez, M.; Jones, S.; Tedrow, J. S. Development and Execution of a Production-Scale Continuous [2 + 2] Photocycloaddition. *Org. Process Res. Dev.* **2020**, *24* (10), 2139−2146.

https://doi.org/10.1021/acs.oprd.1c00240
Org. Process Res. Dev. XXXX, XXX, XXX−XXX